Communication

Chemical#Clathrate Hybrid Hydrogen Storage: Storage in Both Guest and Host

Timothy A. Strobel, Yongkwan Kim, Gary S. Andrews, Jack R. Ferrell III, Carolyn A. Koh, Andrew M. Herring, and E. Dendy Sloan

J. Am. Chem. Soc., **2008**, 130 (45), 14975-14977 • DOI: 10.1021/ja805492n • Publication Date (Web): 17 October 2008

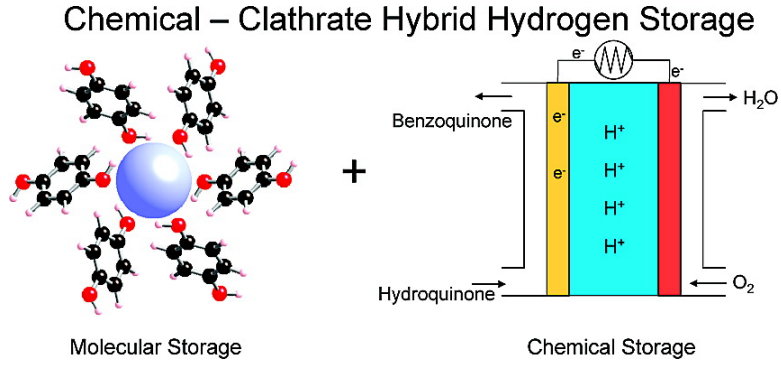

More About This Article

Additional resources and features associated with this article are available within the HTML version:

- Supporting Information
- Access to high resolution figures
- Links to articles and content related to this article
- Copyright permission to reproduce figures and/or text from this article

View the Full Text HTML

J|A|C|S
COMMUNICATIONS

Published on Web 10/17/2008

Chemical−Clathrate Hybrid Hydrogen Storage: Storage in Both Guest and Host

Timothy A. Strobel, Yongkwan Kim, Gary S. Andrews, Jack R. Ferrell III, Carolyn A. Koh, Andrew M. Herring, and E. Dendy Sloan*

Chemical Engineering Department, Colorado School of Mines, Golden, Colorado 80401

Received July 15, 2008; E-mail: esloan@mines.edu

Clathrate compounds are formed from two or more molecular species associated not through strong chemical attraction but through the enclosure of one set of molecules within a suitable structure formed by another.[1] For clathrate hydrates, a crystalline host lattice comprised of hydrogen-bonded water traps small molecules within polyhedral cavities.[2] Recent reports have examined the hydrogen storage potential of different clathrate hydrate structures[3−5] and variants,[6] as well as isomorphous analogues.[7,8] Other types of guest−host materials are also under investigation.[9,10] Simple (one guest) hydrogen clathrate hydrate crystallizes as cubic structure II (sII) with 16 small 5^{12} cavities and 8 larger $5^{12}6^4$ cavities per unit cell. The larger $5^{12}6^4$ cavities may contain up to four hydrogen molecules, while the smaller 5^{12} cavities are limited to a single hydrogen molecule.[11] The maximum H_2 storage of simple hydrogen clathrate hydrate is ∼3.8 wt %.

Unique features such as multiple cavity occupation and H_2-H_2 separation distances smaller than solid hydrogen suggest some potential for clathrates as H_2 storage materials since local densities may be unusually high. Additionally, the ordered nanosized cavities of the clathrate structure provide a unique scenario to study the quantum dynamics of the confined molecules.[12,13]

The practical hydrogen storage in simple sII clathrate hydrate is constrained by severe formation conditions (200 MPa at 273 K).[14] The formation pressure may be significantly reduced with the addition of stabilizing molecules, like tetrahydrofuran (THF),[15] although the storage capacity is also diminished. Currently, the various clathrate hydrate structures can store 1−4 wt % at moderate and more severe pressure conditions, respectively.[16]

The perceived storage limitations of clathrate materials are governed by the amount of hydrogen contained within the cavities relative to the amount of host material/additives present. Here we report a novel concept that alters this perception: hydrogen storage in both the clathrate cavities and the clathrate host lattice. In this work hydroquinone is used for proof-of-concept of the chemical−clathrate hybrid storage.

Hydroquinone (1,4-benzenediol) has three crystalline phases (α, β, γ),[17] with evidence for other pressure-induced phase transitions at 3.3 and 12 GPa.[18] The β phase (β-HQ) has long been known as a clathrate with guest molecules such as hydrogen sulfide and sulfur dioxide.[19] At ambient conditions this molecule crystallizes as α-HQ which consists of rhombohedral needle-like crystals and is favorable in energy by ∼0.13 kcal/mol compared to the empty β-HQ clathrate phase.[20] In the presence of small molecules like methane or xenon, β-HQ is the thermodynamically preferred phase.

The β-HQ clathrate cavities are terminated at the top and bottom by hexagonal $[OH]_6$ rings and surrounded by six C_6H_6 groups, three of which originate from the top $[OH]_6$ ring and three from the bottom (Figure 1).[21] These cavities have a radius of ∼4 Å. Additionally, the standard state of hydroquinone is a crystalline solid, and β-HQ clathrate shows remarkable stability when compared to clathrate hydrates. For example, β-HQ+CH_4 clathrate is stable at 298 K and 0.08 MPa,[22] whereas H_2O+CH_4 clathrate hydrate requires ∼44 MPa at the same temperature. Recently, one molecular dynamics study has investigated the possibility of loading H_2 into the β-HQ clathrate structure.[23]

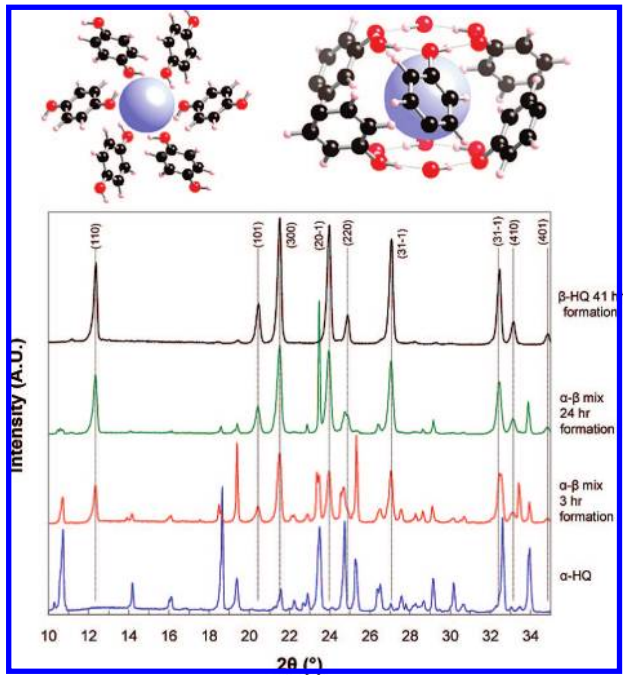

Figure 1. Top: Structure of the β-HQ cavities. Cavity radius is ∼4 Å; hexagonal $[OH]_6$ rings are normal to the *c*-axis of the crystal. Bottom: PXRD patterns at 100 K and atmospheric pressure during β-HQ+H_2 clathrate formation at 296 K and 200 MPa. The starting material was α-HQ (bottom). After 3 h of formation significant amounts of β-HQ Bragg peaks appear in the diffraction pattern. After 41 h the α-HQ has converted to β-HQ (top). Miller indices for β-HQ clathrate are labeled as (*hkl*).

β-HQ+H_2 clathrate was synthesized by pressurizing finely ground α-HQ powder with hydrogen gas at 200 MPa and 296 K. Powder X-ray diffraction (PXRD) patterns taken at different periods during the formation process showed complete conversion to the β-HQ phase in ∼2 days (Figure 1). This formation time can be reduced significantly by pressurizing α-HQ near its melting temperature (440 K) or by forming the clathrate through recrystallization from a supersaturated ethanol solution. The PXRD pattern was indexed to the rhombohedral crystal structure $R\bar{3}$ with $a = 16.595 \pm 0.018$ Å and $c = 5.381 \pm 0.010$ Å, consistent with β-HQ clathrates formed with other small molecules.[19]

β-HQ+H_2 clathrate formation was also observed at much lower pressures, 70 MPa at 296 K, ∼30 MPa less than the required formation pressure for binary THF+H_2 hydrate at 296 K,[15] and ∼700 MPa less than the pressure required for the C_1 H_2+H_2O filled

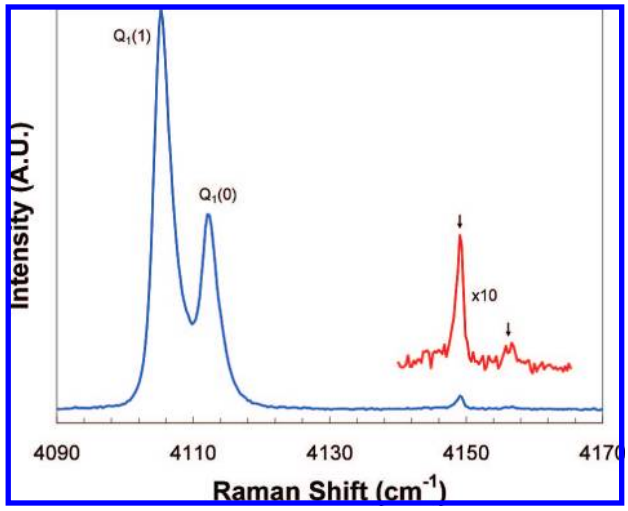

Figure 2. Raman spectrum of the vibron region of β-HQ+H_2 clathrate measured at 76 K and atmospheric pressure. The region around 4150 cm^{-1} has been magnified by a factor of 10, revealing two smaller contributions.

ice phase at this temperature[24] (simple sII H_2 hydrate is not stable above ~273 K at any pressure). The formation pressure of β-HQ+H_2 clathrate may be reduced further by decreasing the formation temperature. When heated slowly from 76 K at atmospheric pressure, the β-HQ+H_2 clathrate did not begin to release H_2 until 230 K, whereas simple H_2 clathrate hydrate starts to release gas above ~80 K and dissociates completely at about ~150 K at atmospheric pressure.[11] Small amounts of hydrogen were observed within the β-HQ clathrate after 30 min of exposure to ambient conditions, and strong H_2 vibron Raman signals were observed from the β-HQ+H_2 clathrate after storage for 7 months in liquid nitrogen.

Raman spectroscopic measurements revealed two distinct H_2 vibron bands at 4105 and 4112 cm^{-1} (Figure 2). These two peaks, which are separated by ~7 cm^{-1}, are assigned to $Q_1(1)$ and $Q_1(0)$ (ortho and para) and followed the expected ortho−para conversion after storage in liquid nitrogen via changes in Raman band intensity.[25] These two bands were significantly red-shifted ($Q_1(1)_{free}$ = 4155 cm^{-1}, $Q_1(0)_{free}$ = 4161 cm^{-1})[26] and broadened compared to the free gaseous phase indicating interactions between H_2 and the host cavities, consistent with the enclathration of hydrogen.[3] Additionally, two weak contributions to the spectrum were observed at 4149 and 4156 cm^{-1}.

Thermodynamic gas release measurements collected after quenching the β-HQ+H_2 clathrate sample in liquid nitrogen revealed the amount of enclathrated hydrogen to be 1.07 ± 0.03 hydrogen molecules per cavity. Based on the value of gas collected being slightly greater than the amount for single occupancy, we assign the intense lower frequency bands at 4105 and 4112 cm^{-1} to the ortho−para contributions of singly occupied cavities and speculate that the higher frequency bands at 4149 and 4156 cm^{-1} are due to small amounts of multiple occupancy, or alternatively, H_2 located in the interstitial sites between connected cavities.

The Raman spectrum of β-HQ+H_2 clathrate in the region of H_2 rotation is complicated by several Raman active modes of hydroquinone (Figure 3). The rotational spectrum was assigned by comparison with β-HQ+D_2 clathrate, where rotational transitions of the heavier D_2 molecule are shifted to lower energy, reflecting the smaller rotational constant. The rotational Raman spectrum revealed that, unlike simple H_2 clathrate hydrate, H_2 molecules confined within β-HQ cavities do not rotate freely. The J=0 → J=2 transition was perturbed around the free gas value (354 cm^{-1})[26]

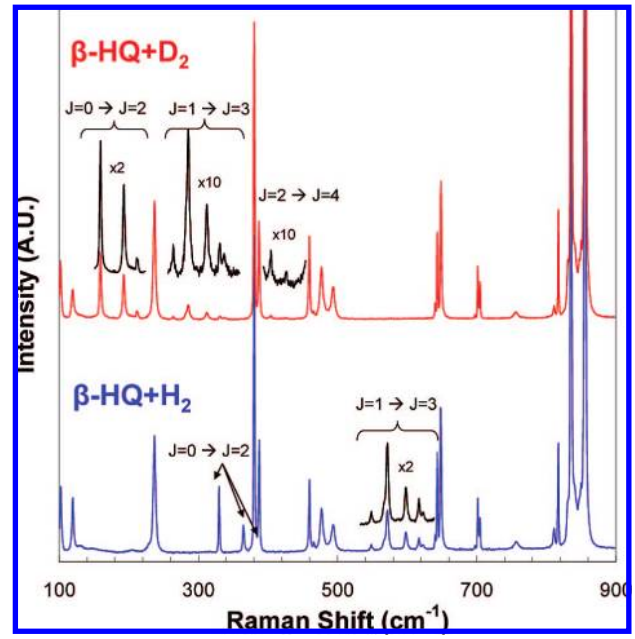

Figure 3. Raman spectra for β-HQ+D_2 (top) and β-HQ+H_2 (bottom) in the region of rotational excitations. The J=0 → J=2, J=1 → J=3, J=2 → J=4 transitions for D_2 and the J=1 → J=3 transition for H_2 have been scaled for clarity. The highest energy band of the J=0 → J=2 triplet for H_2 is coincident with a HQ mode.

up to +31 cm^{-1}, and the J=1 → J=3 transition was perturbed around the free gas value (587 cm^{-1})[26] up to +37 cm^{-1}. Additionally, the spectra revealed that the potential energy surface experienced by the H_2/D_2 molecules in the β-HQ cages is highly anisotropic. The anisotropy of the environment lifts the degeneracy ($2J$+1) of the rotational energy levels. The J=0 → J=2 transition was split into three resolvable bands spread over 54 cm^{-1}, presumably m=0, m=|1|, and m=|2|. The J=1 → J=3 transition is split into at least five resolvable bands spread over 75 cm^{-1}. Two bands were observed for the weaker J=2 → J=4 transition of D_2.

The observed splitting is comparable to the rotational constant for H_2 (59.3 cm^{-1}) and nearly double the rotational constant for D_2 (29.9 cm^{-1}).[26] From the center of the β-HQ clathrate cavity there are two unique nearest neighbor carbon distances as well as two unique nearest neighbor oxygen distances revealing some degree of anisotropy.[21] Splitting of the rotational energy levels from an anisotropic environment is a well-known phenomenon.[12,13,27] However, the currently observed splitting is extremely large when compared with solid hydrogen,[27] clathrate hydrates,[12] or hydrogen carbon systems.[28]

To effectively dehydrogenate the clathrate host lattice, HQ was oxidized to benzoquinone (BQ) directly in a polymer electrolyte membrane fuel cell (PEMFC) to show the first proof-of-principle that the host lattice could be used to power a fuel cell. The driving force for PEMFC operation is based on the overall cell potential comprised of the half-cell reactions at the anode and cathode. The half-cell reactions and redox potentials for HQ[29] and O_2 are shown in eqs 1 and 2, making the overall cell reaction spontaneous.

$$2HQ \rightarrow 2BQ + 4e^- + 4H^+ \quad (E^\circ = -0.699\ V) \qquad (1)$$

$$O_2 + 4e^- + 4H^+ \rightarrow 2H_2O \quad (E^\circ = 1.23\ V) \qquad (2)$$

On the anode side, a 0.66 M aqueous solution of HQ was fed to the PEMFC at 1.2 mL/min. Excess O_2, humidified at 353 K, was supplied at the cathode. The membrane electrode assembly (MEA) consisted of a Nafion 117 membrane and Pt−Ru catalyst

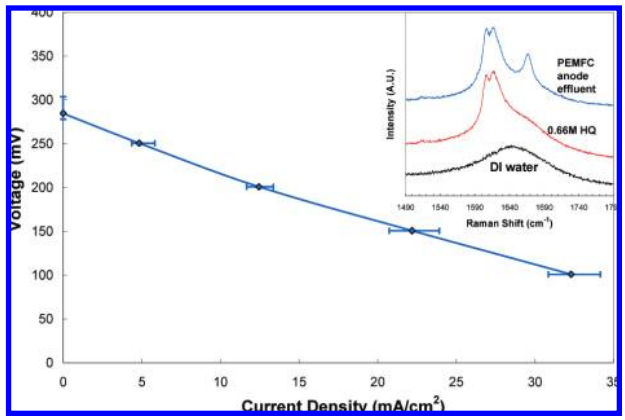

Figure 4. Performance of PEMFC with 1.2 mL/min of 0.66 M HQ operated at 353 K and 2 bar of backpressure. Data points represent the average of data collected over 10 independent experimental scans using the stepwise procedure. Every step for an individual scan consisted of ~246 data points. Error bars represent the total range of data over the >2000 data points collected at a specific voltage. Inset: Raman spectra of deionized water (bottom), 0.66 M HQ solution (middle), and anode side effluent from fuel cell (top). C═O bond stretching is observed at 1668 cm^{-1}.

(4.0 mg/cm^2) supported on carbon at the anode. On the cathode, a carbon-supported Pt catalyst was loaded at 0.5 mg/cm^2. The active area of the MEA was 5.48 cm^2. In measuring the polarization curve, the cell was initialized at open-circuit voltage for 5 min. Following this, the potential was stepped down, in 50 mV increments, by a potentiostat from 250 to 100 mV at 353 K with 2 bar of backpressure.

According to eqs 1 and 2, the theoretical open-circuit voltage is 576 mV. The observed open-circuit voltage of the PEMFC was measured at ~285 mV, and the maximum current density obtained at 100 mV was 32 mA/cm^2 (Figure 4). The difference between the theoretical and observed open-circuit voltage is roughly 300 mV. This difference could be partially explained by reactant crossover from anode to cathode as well as a likely high overpotential to drive the reaction. It should also be noted that the standard reduction potential of HQ varies significantly between one and two electron processes,[29] and the exact mechanism occurring at the anode is unknown. Additionally, interactions between HQ and the carbon support as well as the insolubility of BQ are likely to influence the performance.

The calculated conversion of HQ to BQ at maximum current density was 7%, yielding an effective 0.13 wt % H_2 recovered in the process, although molecular H_2 was not produced as the HQ was used directly. The effluent of the anode side of the fuel cell was analyzed via Raman, confirming the oxidation of hydroquinone to benzoquinone with the evolution of C═O bond stretching at 1668 cm^{-1} (Figure 4 inset). Although the fraction of HQ conversion is low in this system, we demonstrate electrochemical dehydrogenation of the organic host HQ at mild temperature compared with a thermally stimulated process. It should be noted that the PEMFC used was not optimized for this system. It is known that specific catalysts exist that are capable of effectively dehydrogenating hydroquinone.[30] Thus, potential remains for improvement and adaptation to other, higher energy content, molecules.

With one H_2 molecule per cavity, 0.61 wt % hydrogen may be stored in the β-HQ clathrate cavities. When this amount is combined with complete dehydrogenation of the host hydroxyl hydrogens, the maximum hydrogen storage capacity increases nearly 300% to 2.43 wt %. The storage capacity of this particular system falls short of required targets for energy storage, but the concept of using storage from two independent sources of the same material may be revolutionary to hydrogen storage technology. This storage scheme is not limited strictly to clathrate materials, but rather open to a wide variety of compounds. These host compounds should have a suitable mechanism to store molecular hydrogen, such as the hydrogen-bonding motif demonstrated, but must also contain appreciable and accessible chemical energy.

The dehydrogenation of the chemical energy carrier directly within a PEMFC at mild conditions is beneficial to any storage material; however, limitations, such as the crystalline nature and insolubility of HQ, must be overcome. The retrieval of chemical energy could also be obtained by another mechanism, such as a mild thermal decomposition reaction. Finally, the quantum dynamics observed for H_2 contained within the clathrate nanosized cavities provides fundamental insight into the behavior of confined diatomic molecules and valuable experimental data for the theoretical testing of complex intermolecular potentials and rigorous quantum calculations.

Acknowledgment. The authors acknowledge support from the United States Department of Energy under Contract DE-FG02-05ER46242.

References

(1) Powell, H. M. *J. Chem. Soc.* **1948**, 61.
(2) Sloan, E. D. and Koh, C. A. *Clathrate Hydrates of Natural Gases*, 3rd ed.; CRC Press: Boca Raton, FL, 2008.
(3) Mao, W. L.; Mao, H. K.; Goncharov, A. F.; Struzhkin, V. V.; Guo, Q.; Hu, J.; Shu, J.; Hemley, R. J.; Somayazulu, M.; Zhao, Y. *Science* **2002**, *297*, 2247.
(4) Strobel, T. A.; Koh, C. A.; Sloan, E. D. *J. Phys. Chem. B* **2008**, *112*, 1885.
(5) Kim, D. Y.; Lee, H. *J. Am. Chem. Soc.* **2005**, *127*, 9996.
(6) Chapoy, A.; Anderson, R.; Tohidi, B. *J. Am. Chem. Soc.* **2007**, *129*, 746.
(7) van der Berg, A. W. C.; Pescarmona, P. P.; Schoonman, J.; Jansen, J. C. *Chem.—Eur. J.* **2007**, *13*, 3590.
(8) Neiner, D.; Okamoto, N. L.; Condron, C. L.; Ramasse, Q. M.; Yu, P.; Browning, N. D.; Kauzlarich, S. M. *J. Am. Chem. Soc.* **2007**, *129*, 13857.
(9) Culp, J. T.; Natesakhawat, S.; Smith, M. R.; Bittner, E.; Matranga, C.; Bockrath, B. *J. Phys. Chem. C.* **2008**, *112*, 7079.
(10) Thallapally, P. K.; Lloyd, G. O.; Wirsig, T. B.; Bredenkamp, M. W.; Atwood, J. L.; Barbour, L. J. *Chem. Commun.* **2005**, 5272.
(11) Lokshin, K. A.; Zhao, Y.; He, D.; Mao, W. L.; Mao, H. K.; Hemley, R. J.; Lobanov, M. V.; Greenblatt, M. *Phys. Rev. Lett.* **2004**, *93*, 125503.
(12) Ulivi, L.; Celli, M.; Giannasi, A.; Ramirez-Cuesta, A. J.; Bull, D. J.; Zoppi, M. *Phys. Rev. B* **2007**, *76*, 161401.
(13) Xu, M.; Elmatad, Y. S.; Sebastianelli, F.; Moskowitz, J. W.; Bačić, Z. *J. Phys. Chem. B* **2006**, *110*, 24806.
(14) Dyadin, Y. A.; Larionov, E. G.; Manakov, A. Y.; Zhurko, F. V.; Aladko, E. Y.; Mikina, T. V.; Komarov, V. Y. *Mendeleev Commun.* **1999**, *5*, 209.
(15) Florusse, L. J.; Peters, C. J.; Schoonman, J.; Hester, K. C.; Koh, C. A.; Dec, S. F.; Marsh, K. N.; Sloan, E. D. *Science* **2004**, *306*, 469.
(16) Strobel, T. A.; Koh, C. A.; Sloan, E. D. *Fluid Phase Equilib.* **2007**, *261*, 382.
(17) Wallwork, S. C.; Powell, H. M. *J. Chem. Soc., Perkin Trans. 2* **1980**, *12*, 641.
(18) Rao, R. R.; Sakuntala, T.; Arora, A. K.; Deb, S. K. *J. Chem. Phys.* **2004**, *121*, 7320.
(19) Palin, D. E.; Powell, H. M. *J. Chem. Soc.* **1948**, 815.
(20) Evans, D. F.; Richards, R. E. *J. Chem. Soc.* **1952**, 3932.
(21) Mak, T. C. W.; Tse, J. S.; Tse, C. S.; Lee, K. S.; Chong, Y. H. *J. Chem. Soc., Perkin Trans. 2* **1979**, 1169.
(22) van der Waals, J. H.; Platteeuw, J. P. *Adv. Chem. Phys.* **1959**, *2*, 1.
(23) Daschbach, J. L.; Chang, T. M.; Corrales, R.; Dang, L. X.; McGrail, P. *J. Phys. Chem. B* **2006**, *110*, 17291.
(24) Vos, W. L.; Finger, L. W.; Hemley, R. J.; Mao, H. K. *Phys. Rev. Lett.* **1993**, *71*, 3150.
(25) Herzberg, G. *Molecuar Spectra and Molecular Structure I. Diatomic Molecules*; Prentice-Hall: New York, 1939.
(26) Stoicheff, B. P. *Can. J. Phys.* **1957**, *35*, 730.
(27) Van Kranendonk, J. *Solid Hydrogen*; Plenum: New York, 1983.
(28) FitzGerald, S. A.; Yildrium, T.; Santodonato, L. J.; Neumann, D. A.; Copley, J. R. D.; Rush, J. J.; Trouw, F. *Phys. Rev. B* **1999**, *60*, 6439.
(29) Uchimiya, M.; Stone, A. T. *Geochim. Cosmochim. Acta* **2006**, *70*, 1388.
(30) Cowley, S. W.; Ebel, J. E. *Pretreatment of Catalyst Support to Enhance Catalytic Dehydrogenation of a Hydroquinone*; International Publication Number: WO/1996/033015,1996.

JA805492N